

Investigation of Structural, Spectral, Biological Activity of Monohydrous Dihydrogen Phosphate Salt of Ciprofloxacin: Computational and Molecular Docking Study

Siprofloksasinin Monohidröz Dihidrojen Fosfat Tuzunun Yapısal, Spektral, Biyolojik Aktivitesinin Araştırılması: Hesaplamalı ve Moleküler Yerleştirme Çalışması

Tuğba AYCAN¹ , Filiz ÖZTÜRK² , Nilgün ÖZDEMİR³ , Hümeysra PAŞAOĞLU⁴ 

¹ Sinop Üniversitesi, Fizik Bölümü, 57000, Sinop, Türkiye

² Ondokuz Mayıs Üniversitesi, Karadeniz İleri Teknoloji Araştırma ve Uygulama Merkezi, 55139, Samsun, Türkiye

³ Ondokuz Mayıs Üniversitesi, Gıda Mühendisliği, 55139, Samsun, Türkiye

⁴ Ondokuz Mayıs Üniversitesi, Fizik Bölümü, 55139, Samsun, Türkiye

Abstract

The present study describes the synthesis, spectroscopic and biological activity of Monohydrous Dihydrogen Phosphate Salt of Ciprofloxacin (MDPSC). The asymmetrical part of the unit cell contains one ciprofloxacin cation, one dihydrogen phosphate anion and one water molecule. The techniques used for the characterization are single crystal X-ray diffraction and spectroscopic method (IR, UV) and thermal analysis. The molecular structure was theoretically optimized using DFT/B3LYP/6-31G(d,p) methods for ground state, and compared with experimental values. Scaled theoretical vibrational frequencies are compared with experimental values. The UV-Vis results that experimentally obtained are compared with the calculated electronic properties such as HOMO and LUMO energies and the MEP are also investigated. The vibrational frequencies has been studied by comparing the characteristic bands related to the functional groups of the compound and the ciprofloxacin. Thermal properties have been investigated with TGA. Biological study of the complex against Staphylococcus aerous, Escherichia coli, Candida Albicans, Bacillus Subtilis, Pseudomonas aeruginosa and Aspergillus Flavus showed very strong antibacterial activity with MIC values ranging from 512 $\mu\text{g mL}^{-1}$ to 1 $\mu\text{g mL}^{-1}$. The optimized complex is docked to the 5J9B, 5BMM, 5HTG, 1ZUV, 4F0V and 4YNU.

Keywords: Ciprofloxacin, X-ray diffraction, Spectral analysis, Antimicrobial activity, Molecular modelling

Öz

Bu çalışma, Siprofloksasinin Monohidröz Dihidrojen Fosfat Tuzunun (MDPSC) sentezini, spektroskopik ve biyolojik aktivitesini açıklar. Birim hücrenin asimetrik kısmı bir siprofloksasin katyonu, bir dihidrojen fosfat anyonu ve bir su molekülü içerir. Karakterizasyon için kullanılan teknikler, tek kristalli X-ışını kırınımı ve spektroskopik yöntem (IR, UV) ve termal analizdir. Moleküler yapı teorik olarak taban durumu için DFT/B3LYP/6-31G(d,p) yöntemleri kullanılarak optimize edildi ve deneysel değerlerle karşılaştırıldı. Ölçekli teorik titreşim frekansları deneysel değerlerle karşılaştırıldı. Deneysel olarak elde edilen UV-Vis sonuçları, HOMO ve LUMO enerjileri ve MEP gibi hesaplanan elektronik özelliklerle karşılaştırıldı. Titreşim frekansları, bileşiğin ve siprofloksasinin fonksiyonel gruplarıyla ilgili karakteristik bantların karşılaştırılmasıyla çalışılmıştır. TGA ile termal özellikler incelenmiştir. Kompleksin Staphylococcus aerous, Escherichia coli, Candida Albicans, Bacillus Subtilis, Pseudomonas aeruginosa ve Aspergillus Flavus'a karşı yapılan biyolojik çalışma, MIC değerleri 512 $\mu\text{g mL}^{-1}$ ila 1 $\mu\text{g mL}^{-1}$ arasında değişen çok güçlü bir antibakteriyel aktivite göstermiştir. Optimize edilmiş kompleks, 5J9B, 5BMM, 5HTG, 1ZUV, 4F0V ve 4YNU'ya yerleştirilmiştir.

Anahtar Kelimeler: Siprofloksasin, X ışını kırınımı, Spektral analiz, Antimikrobiyal aktivite, Moleküler modelleme

Sorumlu yazar/Corresponding Author: Tuğba AYCAN, Tel: 0(368) 271 57 79, e-posta: taycan@sinop.edu.tr

Gönderilme/Submitted: 21.06.2019, **Düzenleme/Revised:** 26.10.2019, **Kabul/Accepted:** 11.12.2019

I. INTRODUCTION

Fluoroquinolone is a broad spectrum synthetic antibiotic that are quinolone members. These antibiotics show antimicrobial effects by acting as natural molecules in the cell. At the same time, fluoroquinolones are known as chemotherapeutic agents [1]. Research of crystals as antibiotics has drawn great interest for many years and the number of these studies has showed increase. The different designs of fluoroquinolone molecules have resulted in compounds with a new biological effect [2]. Ciprofloxacin cation with acceptor and donor groups can participate in the formation of hydrogen bonds. The compounds can crystallize in a variety of polymeric forms as well as in co-crystals, salts, and crystal hydrates and solvates as the components of complexes [3]. While an organic acid can be more preferred than a simple drug molecule, phosphoric acid which is an inorganic acid displays H-bond pattern in the formation of mix-ligand crystals [2]. There are few quantum chemical analyses on ciprofloxacin. Recently some quantum chemical studies have been made on ciprofloxacin. In this study, firstly monohydrous dihydrogen phosphate salt of ciprofloxacin was synthesized, its structural (Single Crystal XRD) and spectral (TGA, IR and UV-VIS) analyses were done together with theoretical calculations at the same time. Molecular electrostatic potential (MEP) maps were investigated and some quantum chemical parameters were theoretically calculated for the biological reactivity of complex. We aimed to improve the biological and pharmaceutical properties of antibacterial ciprofloxacin used in treatment. In addition to this analysis, the complex was docked to appropriate proteins taken from Protein Data Bank (<http://www.rcsb.org/pdb/home/home.do>).

II. MATERIAL AND METHODS

2.1. Synthesis

A mixture of 0.5 mmol ciprofloxacin (0.19 g), and 0.2 mmol phosphoric acid (0.020 g) and H₂O (20 ml) was heated until dissolved and colorless crystals were obtained after several days. Washed with distilled water and finally dried in air.

2.2. Physical Measurements

By preparing KBr pellet disc, in the mid-IR region (4000-400 cm⁻¹), the IR spectrum was recorded by a Bruker Vertex 80V FT-IR spectrometer and to converted from absorbance to transmittance using Bruker OPUS software. MFMF (the magnetic field modulation frequency) and the microwave power were regulated as 100 kHz and 0.998 mW,

respectively. At room temperature, the UV-Visible spectrum in aqua solution was recorded by a Unicam UV-Vis spectrometer between 190 and 1100 nm. The absorption spectra of title complex was drawn using VISIONcollect Software. Simultaneous TG, DTG and DTA curves were obtained in nitrogen atmosphere at 10 K/min heating rate in the platinum pats, in the range of temperature 20-1000 °C by using TA/DMAQ800 thermal analyser in OMU-KITAM laboratory. XRD data was collected using a Stoe IPDS diffractometer at 296 K by graphite monochromatic MoK_α radiation ($\lambda=0.71073 \text{ \AA}$). The crystal structure was analyzed by direct methods and all non-hydrogen atoms were refined anisotropically by full matrix least-squares methods using the program SHELX2008 [4]. WinGX [5], ORTEP-3 for Windows [5] and MERCURY [6] software were used for molecular drawings and other materials. Crystal data and structure refinement parameters are given in Table 1.

Table 1. Crystal data and structure refinement parameters for complex

Formula	C ₁₇ H ₂₃ N ₃ O ₈ FP
Formula weight	447.35
Temperature(K)	296
Radiation, λ (MoK _α)	0.71069
Crystal system	Triclinic
Space group	P-1
Unit cell dimensions	
a, b, c (Å)	7.401 (5), 9.046 (5), 15.858 (5)
α , β , γ (°)	100.398 (5), 97.630 (5), 107.004 (5)
Volume (Å ³)	979.0 (9)
Z	2
Calculated density (g cm ⁻³)	1.518
μ (mm ⁻¹)	0.20
F(000)	468
Crystal size (mm)	0.25×0.20×0.10
θ range (°)	1.3-27.2
Index ranges	-9≤h≤9 -11≤k≤10 -20≤l≤20
Measured Reflections	7098
Independent reflections	3920
Reflections observed [I ≥ 2σ(I)]	3007
Absorption correction	Integration
Refinement method	Full matrix least-squares on F ²
Data/restraints/parameters	3920/0/307
Goodness-of-fit on F ²	1.07
Final R indices [I ≥ 2σ(I)]	R ₁ =0.044; wR ₂ =0.130
R indices (all data)	0.069

2.3. Antibacterial Activity

The antimicrobial activity of the complex and the sole ligand against *Staphylococcus aureus* ATCC 33862 (gram+),

Bacillus subtilis NRRL-B 209 (gram+), *Pseudomonas aeruginosa* ATCC 27853 (gram-) and *Escherichia coli* ATCC 25922 (gram-) bacteria, *Candida albicans* ATCC 10131 yeast and *Aspergillus flavus* MAM 200682 fungi was determined as minimum inhibitory concentrations (MIC) by the micro dilutions technique (96-well microplates technique) using the National Committee for Clinical Laboratory Standards (NCCLS) recommendations [7, 8]. In this assay, it was used Mueller–Hinton broth (Merck) for the bacterial strains and RPMI 1640 broth (Merck) for the fungal and yeast strains as growth medium. Serial twofold dilutions of standard and analyzing compounds ranging from 512 $\mu\text{g mL}^{-1}$ to 1 $\mu\text{g mL}^{-1}$ concentration were prepared in mediums. And these dilutions were added as 100 μL in each well of a 96-well microplate. For inoculum of microorganisms, it was prepared adjusted to a turbidity equivalent to a 0.5 Mc Farland standard by using a 24 h culture of yeast strains and 18 h broth culture of each bacteria. A final concentration of 5×10^5 CFU mL^{-1} for bacteria and 0.5×10^3 to 2.5×10^3 CFU mL^{-1} for yeast in the microplate were diluted in broth media to give. Then the microplates were incubated at 35 °C for 20 h for bacteria, at 25 °C for 48 h for yeast and 25 °C for 72–96 h for fungal cultures.

2.4. DFT and Molecular Modelling

Density functional theory (DFT) calculations were applied by using Gaussian-09 software [9]. The minimum energy molecular geometry of the complex was predicted by B3LYP hybrid method. Geometric optimization was carried out at 6-31G(d,p) level. Molecular docking is a key tool in structural molecular biology and computer-aided drug design. The crystal structure *Staphylococcus aerous*, *Escherichia coli*, *Candida Albicans*, *Bacillus Subtilis*, *Pseudomonas aeruginosa* and *Aspergillus Flavus* were downloaded from the protein Data Bank (PDB ID: 5J9B, 5BMM, 5HTG, 1ZUV, 4F0V and 4YNU, respectively, <http://www.rcsb.org/pdb>). The molecular docking studies were performed by AutoDock Tool (ADT) v1.5.6 and AutoDock Vina docking software. By AutoDock Tool software, to protein residues, polar hydrogen atoms were added. Precalculated atomic affinity grid map was constituted for each atom type in the ligand by AUTOGRID. The grid box of $x \times x$ (Å) is with spacing of 1 Å. The interactions between the complex and proteins are carried out by Discovery Studio Visualizer software.

III. RESULTS AND DISCUSSION

3.1. X-ray Study and Optimized Geometry

The molecule has four molecules per unit cell ($Z = 2$) and the space group $P-1$. From SCXRD data results, it is

studied out that the crystal has triclinic by having to the following unit cell dimensions; $a=7.401(5)$ Å, $b=9.046(5)$ Å, $c=15.858(5)$ Å and the angles of $\alpha=100.398(5)^\circ$, $\beta=129.296(5)^\circ$, $\gamma=107.004(5)^\circ$. The asymmetrical part of the unit cell contains one ciprofloxacin cation, one dihydrogen phosphate anion and one water molecule (Figure 1). In the crystal structure, a hydrogen atom is transferred from phosphoric acid to the nitrogen atom in the piperazine ring of ciprofloxacin. Due to these transfer, the changes are observed in the bond lengths of the piperazine ring and carboxylic acid group in the ciprofloxacin cation. However, bond lengths of cyclopropyl group do not show in any change. The N1–C10, C2–C10 and O1–C1 bond length in complex is shorter than that of ciprofloxacin complex N1–C10, C2–C10 and O1–C1. N13–C15, N3–C16 and C16–C17 bond length in complex is longer than that of ciprofloxacin complex N13–C15, N3–C16 and C16–C17 (Table 2) [10]. The reason why of these changes in bond lengths, O and H atoms can be attended to the hydrogen bonding. In the complex, while the shortening in the bond lengths of the carboxylic acid group is about 0.01 Å, there are considerable extensions in the bond lengths of the piperazine ring (0.44-0.23 Å). The strong hydrogen bond made between O atom of phosphoric acid anion and N atom of the piperazine ring causes elongation of bond lengths of N3–C16 and N3–C17.

The crystal packing of the compound is achieved by intra and intermolecular hydrogen bonds. The hydrogen bond geometry is given in Table 3. The N atom in the piperazine ring of ciprofloxacin cation are bound to O atoms of the phosphate anions by the $\text{N3—H3A} \cdots \text{O7}^{\text{vii}}$ and $\text{N3—H3B} \cdots \text{O6}^{\text{viii}}$ hydrogen bonds resulting in a centrosymmetric $R_4^4(12)$ motif (Figure 2). As well as another $R_4^4(12)$ ring motif is formed by the hydrogen bond interaction between the water molecule and phosphate anion ($\text{O8—H7A} \cdots \text{O6}^{\text{iv}}$ and $\text{O4—H4} \cdots \text{O8}^{\text{ii}}$) (Figure 3). These intermolecular hydrogen bonds play an important role in the formation of 3D supramolecular structure of complex. The observed and calculated bond lengths, bond angles for the complex are listed in Table 2. The theoretical values of the geometric parameters are almost in accord with experimental values in despite of small differences (Figure 4). These differences are due to ignored molecular interactions in the gas phase. When the agreement between experimental and theoretical geometric parameters is examined, r.m.s.d is 0.145. These value showed that optimized and experimental structure are rather corresponded.

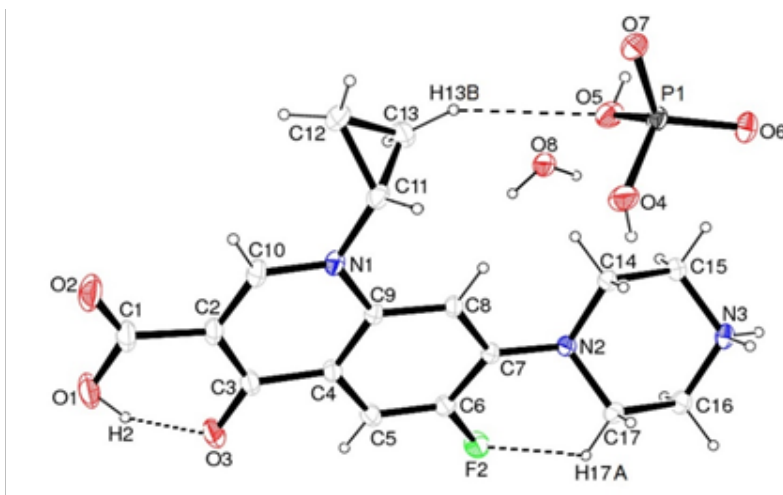


Figure 1. Ortep 3 diagram for monohydrated dihydrogen phosphate salt of ciprofloxacin, with the atom numbering scheme (The intramolecular hydrogen bonds are shown with dashed lines)

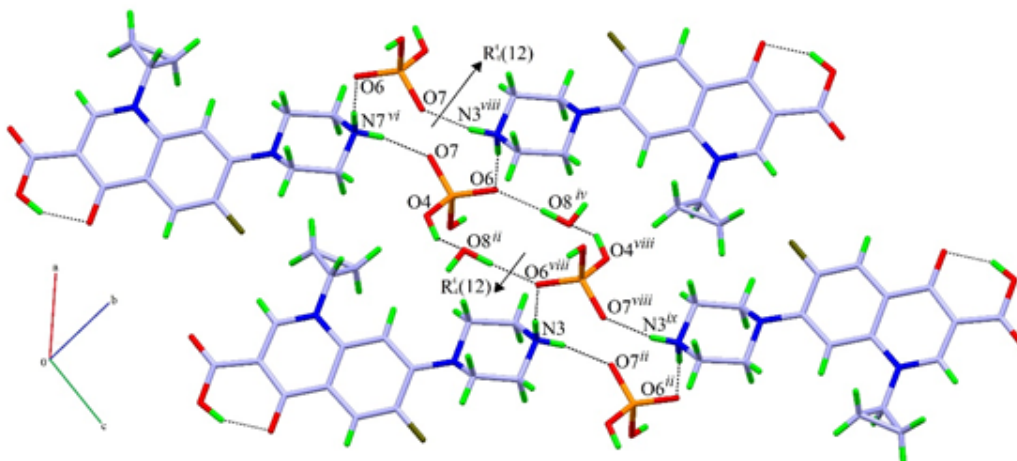


Figure 2. A partial packing diagram with O4 – H4...O8ⁱⁱ intermolecular hydrogen bonds

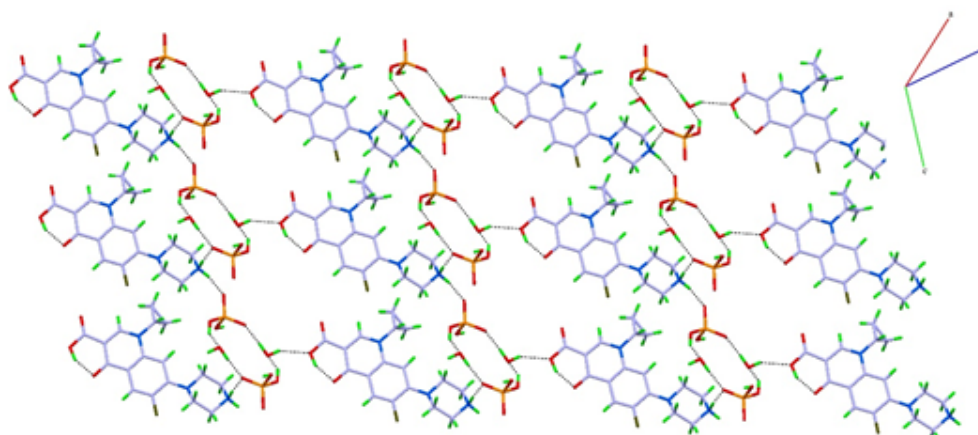


Figure 3. The two-dimensional plane by hydrogen bonds formed among phosphate anions, water molecules and carboxylic acid groups along the [110] direction

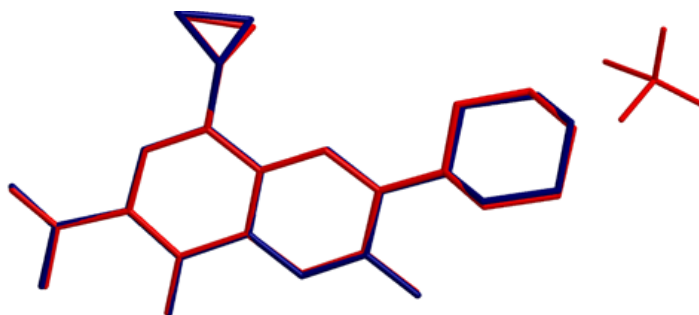


Figure 4. The image of superimposition of the experimental (red) and calculated (black) structures of the title molecule

Table 2. Selected bond distances (Å), angles (°) obtained by X-ray and DFT/B3LYP/6-31G(d,p).

	Experimental	DFT/6-31G(d,p)
Bond lengths (Å)		
P1–O4	1.5644 (17)	1.631
P1–O5	1.551 (2)	1.618
P1–O6	1.4903 (16)	1.483
P1–O7	1.5025 (17)	1.575
F2–C6	1.348 (3)	1.356
N1–C10	1.335 (3)	1.357
C2–C10	1.360 (3)	1.368
C10–H10	0.91 (3)	1.08
O1–C1	1.321 (4)	1.334
O1–H2	0.91 (4)	0.996
C11–C12	1.481 (3)	1.504
C13–C12	1.482 (4)	1.506
N3–C16	1.479 (3)	1.479
N3–C15	1.486 (3)	1.480
Bond angles (°)		
O2–C1–O1	121.5 (2)	122.719
O1–C1–C2	114.8 (3)	115.269
F2–C6–C5	118.44 (19)	119.402
F2–C6–C7	118.14 (17)	117.935
N1–C11–C12	118.9 (2)	119.697
N1–C11–C13	117.7 (2)	119.887

Table 3. Hydrogen bonding geometry for the title compound

<i>D</i> –H... <i>A</i>	<i>D</i> –H	H... <i>A</i>	<i>D</i> ... <i>A</i>	<i>D</i> –H... <i>A</i>	
O5–H5...O7 ⁱ	0.82	2.05	2.558 (2)	119	– <i>x</i> +1, – <i>y</i> , – <i>z</i> +1
O4–H4...O8 ⁱⁱ	0.82	2.11	2.642 (3)	123	<i>x</i> +1, <i>y</i> , <i>z</i>
C12–H12 <i>B</i> ...O2 ⁱⁱⁱ	0.97	2.42	3.220 (3)	139	– <i>x</i> , – <i>y</i> –1, – <i>z</i>
O8–H7 <i>A</i> ...O6 ^{iv}	0.96 (4)	1.74 (4)	2.694 (3)	176 (3)	– <i>x</i> +1, – <i>y</i> +1, – <i>z</i> +1
O8–H7 <i>B</i> ...O1 ^v	0.81 (4)	2.16 (4)	2.900 (3)	151 (3)	– <i>x</i> , – <i>y</i> , – <i>z</i>
C10–H10...F2 ^{vi}	0.91 (3)	2.52 (3)	3.288 (3)	143 (2)	<i>x</i> , <i>y</i> –1, <i>z</i>
N3–H3 <i>A</i> ...O7 ^{vii}	0.88 (3)	1.87 (3)	2.731 (3)	166 (2)	<i>x</i> , <i>y</i> +1, <i>z</i>
N3–H3 <i>B</i> ...O6 ^{viii}	0.94 (4)	1.76 (4)	2.690 (3)	172 (3)	– <i>x</i> +2, – <i>y</i> +1, – <i>z</i> +1
C17–H17 <i>A</i> ...F2	0.97	2.24	2.888 (3)	123	
C13–H13 <i>B</i> ...O5	0.97	2.63	3.517 (3)	152	
O1–H2...O3	0.91 (4)	1.68 (4)	2.528 (3)	153 (4)	

3.2. FT-IR Spectra

The infrared spectra experimental and theoretical for the complex was given in Figure 5. Moreover, the calculated and experimental vibration frequencies of compound are given by comparing in Table 4. Since the vibrational frequencies carried from experimental results are generally smaller than their DFT calculation, to match the theoretical results with experimental those, empirical scaling factors are used [11]. The theoretical vibrational frequencies were calculated at B3LYP/6-31G(d,p) level and scaled by 0.9627 [12]. The scaled theoretical frequencies are found as agreeable with the experimental FT-IR spectrum. The OH stretching vibrations lied in the region 3500–3000 cm^{-1} in FT-IR spectrum are considerably effected from inter and intramolecular hydrogen bonds. The broad peak appeared at 3504 cm^{-1} origins from the stretching vibration of the water molecule. Moreover, shoulder at 3423 cm^{-1} is assigned to stretching vibration of OH groups [13]. While the $\nu(\text{NH})$ stretching vibration of the piperazine ring in the free ciprofloxacin ligand is shown at 3143 cm^{-1} , this peak is not present in the spectrum of new complex. The reason is that, one H atom transfers from phosphoric acid to the piperazine ring of ciprofloxacin. So the new vibration bands are seen at 3080 cm^{-1} and 3050 cm^{-1} because of the NH_2^+ stretching vibration on

the piperazine ring. This is consistent with X-ray diffraction results. The bands observed at 1721 cm^{-1} and 1630 cm^{-1} can be assigned to the stretching vibrations of carboxylic $\nu(\text{C}=\text{O})$ and the phenyl part $\nu(\text{C}=\text{O})$, respectively [14, 15]. The stretching vibrations $\nu(\text{CH})$ of phenyl groups and the other $-\text{CH}_2$ groups in the complex were observed between 3027 cm^{-1} and 2855 cm^{-1} , respectively. These values correspond with by the expected values [13, 16]. The stretching bands at 1274 cm^{-1} , 1164 cm^{-1} and 1144 cm^{-1} were assigned to the $\nu(\text{C}-\text{C})$, $\nu(\text{C}-\text{N})$ and $\nu(\text{C}-\text{O})$, respectively [16].

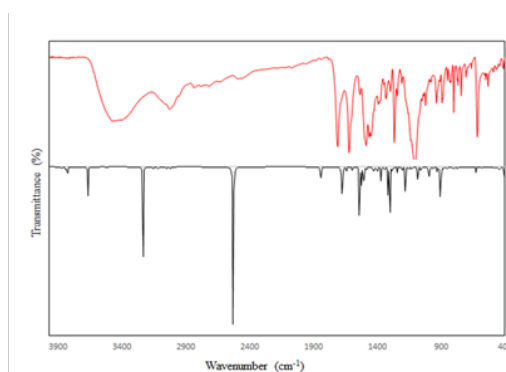


Figure 5. Experimental (red) and calculated (black) FT-IR spectrum of the complex

Table 4. The characteristic experimental vibrational assignments and corresponding calculated values (cm^{-1})

Assignments	Ciprofloxacin [7-10]	Complex (exp.)	Complex (calcd.)
$\nu(\text{H}_2\text{O})$	-	3504 broad	3868,3665
$\nu(\text{OH})$	3490-3450	3423sh	3836, 3822
$\nu(\text{NH})$	3143	-	-
$\nu(\text{NH})_{\text{NH}_2^+}$	-	3080w,3050m	3516, 2524
$\nu(\text{CH})-\nu(\text{CH}_2)$	3086-2909	3027-2855	3268-3235, 3159-3016
$\nu(\text{C}=\text{O})_{\text{COOH}}$	1724	1721s	1835
$\nu(\text{C}=\text{O})_{\text{phenyl}}$	1616	1630s	
$\delta(\text{H}_2\text{O})$	-	1609sh	1683-1638
Phenyl breathing		1546 w	
$\delta(\text{NH})$	1590	-	-
$\delta(\text{C}=\text{C})$			1591,1534
$\delta(\text{OH})$	1542-1443	1508-1459	1531
$\delta(\text{CH})-\delta(\text{CH}_2)$			1526-1504
$\delta(\text{NH})$	1374s	-	-
$\delta(\text{NH})_{\text{NH}_2^+}$	-	1400w,1390w	1478, 1425
$\delta(\text{CH}_2)$	1330,1310	1339s,1305s	1478-1397
$\nu(\text{C}-\text{C})$	1286	1274vs	1361
$\nu(\text{C}-\text{N})$	1184	1164w	1278
$\nu(\text{C}-\text{O})$	1146	1144 sh	1266
$\gamma(\text{CH}_2)$	1115w	1113vs	1261-1242
$\nu(\text{C}-\text{F})$	1037	1056	1197
$\gamma(\text{NH})_{\text{NH}_2^+}$	-	1028	1144
$\gamma(\text{CH})$	988,959	991w,982w	1122
$\delta(\text{COO}^-)$	775-709	778-708	893-732
Ring deformation	652-544	666-534	707-625

(as: asymmetric; s: symmetric; ν : stretching; δ : in plane; γ : out of plane, vs: very strong; s: strong; m: medium; w: weak; sh: shoulder.)

3.3. Chemical Activity

Conjugated molecules are described by the gap between the highest occupied molecular orbital (HOMO) and the lowest unoccupied molecular orbital (LUMO). The gap between E_{HOMO} and E_{LUMO} is important to the molecular chemical stability. Moreover, by using E_{HOMO} and E_{LUMO} values of a molecule, the global chemical reactivity of molecules describe in Table 5 [17]. The parameters of the complex were compared with that of ciprofloxacin, norfloxacin [1] and levofloxacin [1] in Table 5. GaussSum 3.0 Software [18] was used to investigate the properties of frontier molecular orbitals and to plot TDOS shown in Figure 6.

Table 5. Calculated quantum chemical descriptors of complex, ciprofloxacin, norfloxacin and levofloxacin at same level of theory

DFT	Complex	Ciprofloxacin	Norfloxacin [1]	Levofloxacin [1]
E_{HOMO}^a	-6.49	-6.05	-7.74	-7.45
E_{LUMO}^a	-1.92	-1.59	-1.11	-1.08
E_{GAP}^a	4.57	4.46	6.63	6.37
I^a	6.49	6.05	7.74	7.45
A^a	1.92	1.59	1.11	1.08
η^a	2.29	2.23	3.31	3.19
σ^b	0.44	0.45	0.30	0.31
χ^a	4.21	3.82	4.43	4.26
CP^a	-4.21	-3.82	-4.43	-4.26
ω^a	3.87	3.27	2.96	2.85
N^b	0.26	0.31	0.34	0.35
ΔN_{MAX}^b	1.84	1.71	1.34	1.34
S^b	0.22	0.22	0.15	0.16

(^a:eV; ^b:eV⁻¹; I:ionization energy, A:electron affinity, η :absolute hardness; σ :absolute softness; χ :absolute electronegativity; CP:chemical potential; ω :electrophilicity index; N:nucleophilicity index; ΔN_{MAX} :additional electronic charges; S:global softness)

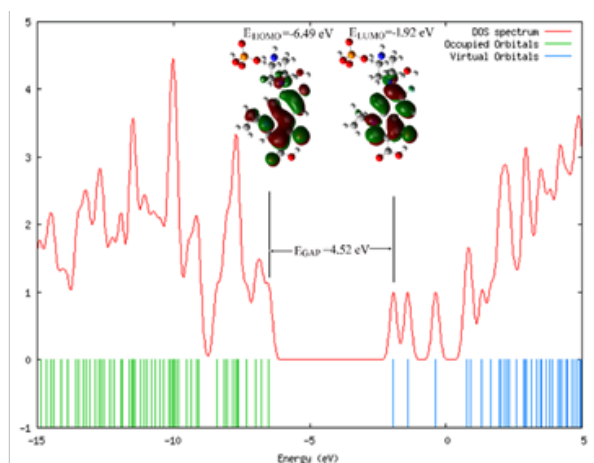


Figure 6. Calculated total density of the states (TDOS) spectrum of the MDPSC

As the E_{HOMO} value increases, the reactivity of the compound increases, while the biological value of the compound increases with decreasing E_{LUMO} value. The complex exhibits higher biological activity in comparison with norfloxacin and levofloxacin and ciprofloxacin exhibits higher biological activity with regard to the complex. The MEP map of the molecule showed that while the around of the oxygen atom is the most electronegative region (red color), the amino groups and the H atoms are electropositive (blue color) because of the electron-donating nature of the amino groups (Figure 7).

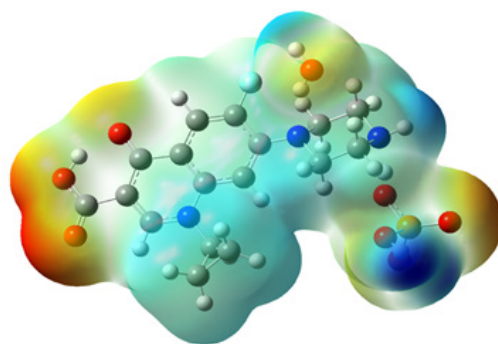


Figure 7. The visual of MEP map calculated at DFT/B3LYP/6-31G (d,p) level

3.4. Electronic Absorption Spectra

The UV-Vis spectrum of the complex and ciprofloxacin in water was recorded within 190-1100 nm range. Moreover, electron transition between energy levels of these compounds have been studied with TD-DFT method. The UV-Vis absorption data were calculated using the GaussSum 3.0 software program [18]. There are characteristic absorption bands in the UV-Vis spectra of ciprofloxacin [19]. The bands observed between about 200 nm and 280 nm are due to the $\pi \rightarrow \pi^*$ transition in the aromatic ring. When the calculated values of the $\pi \rightarrow \pi^*$ transition (Cipro: 219 nm, 244 nm and 277 nm; Complex: 228 nm, 245 nm and 272 nm) are compared with the experimental values (Cipro:218 nm, 249 nm and 277 nm; Complex: 221 nm, 245 nm and 275 nm), it is found that the results are in good agreement with the calculated values. These values may slightly shift due to solvent effect. The maxima at 335 nm and 341 nm observed in the experimental UV-Vis spectrum of ciprofloxacin and the complex, respectively, are due to the $n \rightarrow \pi^*$ transition. However, these values are not observed in the theoretical UV-Vis spectrum. While there are solvent and intermolecular hydrogen bonding effects in the experimental spectrum, these effects have been neglected in the theoretical calculation. The emergence of the new absorption band at 365 nm observed in complex solution with deprotonable groups may

be due to structural changes of the –COOH group. That is, one of the O atoms can be protonated and the other can be bonded to the 4-keto group (Figure 8) [10].

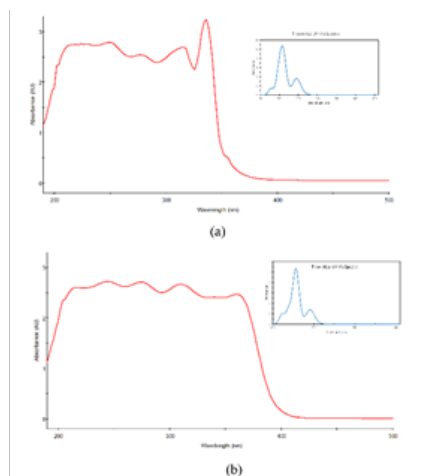


Figure 8. Experimental and theoretical UV-Vis spectra of (a) ciprofloxacin and (b) MDPSC

3.5. Thermal Analysis

The thermal analysis curve of $[\text{HCip} \cdot \text{H}_2\text{PO}_4 \cdot \text{H}_2\text{O}]$ complex is given in Figure 9. At a temperature range of 20-90 °C, a mole water molecule in the complex is disintegrated endothermically. At this stage, a mass reduction of 4.06% occurs (DTG_{max} : 45 °C; calcd: 4.02%). The resulting complex loses 45% of the mass at a temperature range of 250-888 °C, which is attributed to a part of the ciprofloxacin cation. In the last step, an endothermic decomposition (DTG_{max} : 970 °C) occurs at a temperature range of 888-1000°C. It seems that the decomposition continues up to higher temperatures than this temperature.

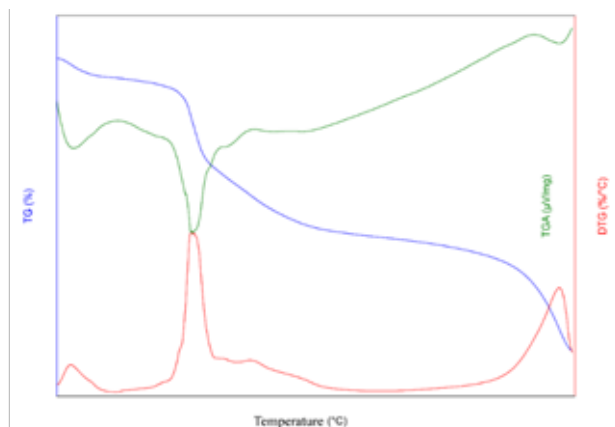


Figure 9. The thermogravimetric curves of complex

3.6. Biological Activity

Ciprofloxacin is an antibiotic that is used to treat bacterial infections. It stops the multiplication of bacteria by

inhibiting the reproduction and repair of their genetic material (DNA). Ciprofloxacin bind to the A subunit of DNA gyrase, which maintains the ordered structure of the chromosome 22 inside the cells [20, 21]. In the current study, minimal inhibitory concentration (MIC) of the ciprofloxacin and its complex were established for a lot of microorganisms and the results were shown in Table 6.

Table 6. MIC values of ciprofloxacin and complex

Compounds	Microorganisms					
	<i>S. aureus</i>	<i>B. subtilis</i>	<i>P. aeruginosa</i>	<i>E. coli</i>	<i>C. albicans</i>	<i>A. flavus</i>
Ciprofloxacin	>512	1	1	1	8	128
Complex	>512	1	1	128	64	>512

The MIC values of the complex against all tested microorganisms differed. Especially, it was determined that the complex had a significant antimicrobial activities with MIC value of 1 $\mu\text{g mL}^{-1}$ against *P. aeruginosa* ATCC 27853 and *Bacillus subtilis* NRRL-B 209 strains. However, it was observed that the antimicrobial activities of the sole ligand against same pathogenic microorganisms. Another important MIC value was 64 $\mu\text{g mL}^{-1}$ and against *Candida albicans* ATCC 10131. But, MIC value of the ligand was 8 times higher than the complex. Among other pathogenic bacteria strains, the antimicrobial activity shown against *Escherichia coli* ATCC was determined as weaker (128 $\mu\text{g mL}^{-1}$) than that of ligand. In the study conducted by Tan, Tan [22], it was investigated antimicrobial activity of ciprofloxacin complexes with the Cu^{2+} , Mn^{2+} and Zr^{2+} metal ions against same strain of *P. aeruginosa*, and determined that MIC values changed in the range of 32 and >128 $\mu\text{g mL}^{-1}$. Therefore, this shown that ciprofloxacin complex with H_2PO_4 was more effective than ciprofloxacin complexes with metal ions.

3.7. Docking Study

Molecular docking is an efficient application in order to obtain an idea about receptor-ligand interactions, geometries, inhibition constants, and binding affinities. It is process that strive to find the best relation between a protein and a ligand. When ligands bind to the protein, the interaction energies arise and the order of these energies is 5J9B=5BMM=1ZUV>4YNU>5HTG=4F0V according to proteins ID (Table 7). Binding energy and inhibition constant are as shown in Table 8. Inhibition constant (K_i) is a measure of binding affinity between the complex and the protein. It is calculated by $\Delta G_B = RT \cdot \ln K_i$. K_i is important to predict how much a ligand can inhibit a protein and interact with a substrate. The smaller the K_i value, the less the patient need the drug to inhibit the enzyme activity. According

to molecular docking results, it is seen that complex without H_3PO_4 interact better with *S. aerous*, *E. coli* and *B. Subtilis*

than the other bacteria. The docked complexes are presented in Figure 10.

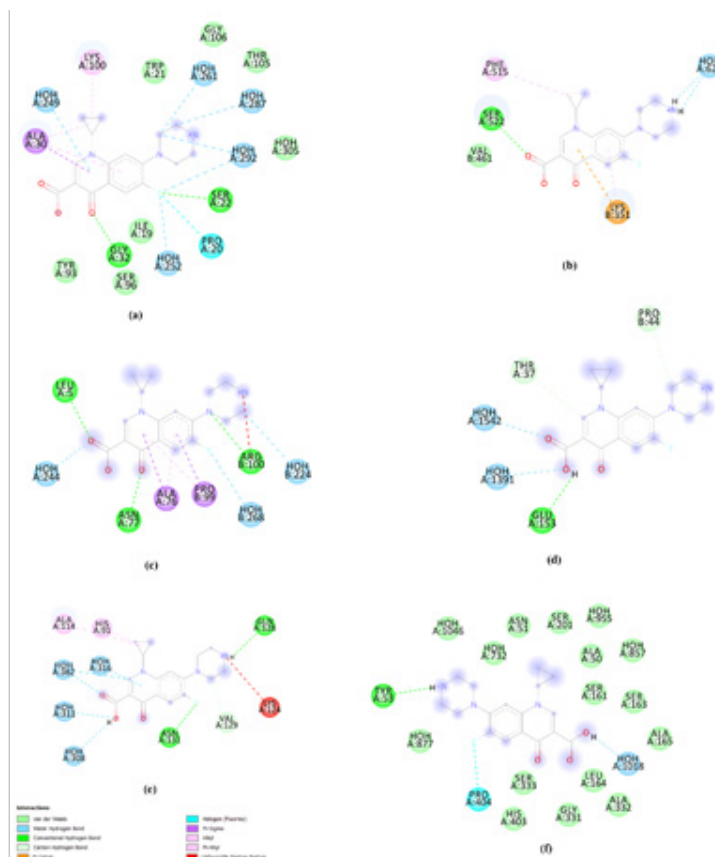


Figure 10. 2D diagram of ligand-protein interactions, docking complex with (a) 5J9B (b) 5BMM (c) 5HTG (d) 1ZUV (e) 4F0V (f) 4YNU

Table 7. Docking energies for complex-protein receptor

Protein ID	Free Energy of Binding $\Delta G_B \Delta G_B$ (kcal mol ⁻¹)	Inhibition Constant, K_i (μ M)
5J9B	-7.2	5.646
5BMM	-7.2	5.646
5HTG	-6.0	42.310
1ZUV	-7.2	5.646
4F0V	-6.0	42.310
4YNU	-6.7	13.037

IV. CONCLUSION

In the current study, Monohydrus Dihydrogen Phosphate Salt of Ciprofloxacin [$HCip.H_2PO_4.H_2O$] was mainly investigated structural characterization and spectroscopic properties. The minimum energy of structure is calculated and geometric parameters were investigated. It is observed that optimized structure is corresponded to the experimental structure which by 0.145 rmsd value. In the complex, due to transferring a hydrogen atom from phosphoric acid to the nitrogen atom in the piperazine ring, the changes in the bond

lengths of the piperazine ring and carboxylic acid group are observed. This transfer is supported by appearance of NH_2 band instead of NH band in the IR spectrum. By the hydrogen bond interaction, $R_4^4(12)$ ring motifs are observed and 3D supramolecular structure is formed by these rings. Generally, the ciprofloxacin was showed higher antimicrobial activity than the complex. When antibacterial and molecular modelling results are compared, molecular docking studies are in rapport with antibacterial assay.

Acknowledgment

Financially, Ondokuz Mayıs University has supported this study (Project No: PYO.FEN.1904.15.022).

REFERENCES

- [1] Sayin, K., Karakaş, D., Kariper, S.E., & Sayin, T.A. (2018). Computational study of some fluoroquinolones: Structural, spectral and docking investigations. *Journal of Molecular Structure*, 1156, 172-181.
- [2] Lou, B., Boström, D., & Velaga, S.P. (2007). Monohydrated dihydrogen phosphate salts of norfloxacin and ciprofloxacin. *Acta Crystallographica Section C: Crystal Structure Communications*, 63(12), o731-o733.
- [3] Blokhina, S., Sharapova, A., Ol'khovich, M., & Perlovich, G. (2017). Sublimation thermodynamics of four fluoroquinolone antimicrobial compounds. *Journal of Chemical Thermodynamics*, 105, 37-43.
- [4] Sheldrick, G.M. (2008). A short history of SHELX. *Acta crystallographica. Section A, Foundations and Advances*, 64(1), 112-122.
- [5] Farrugia, L.J. (2012). WinGX and ORTEP for Windows: an update. *Journal of Applied Crystallography*, 45(4), 849-854.
- [6] Macrae, C.F., Edgington, P.R., McCabe, P., Pidcock, E., Shields, G.P., Taylor, R., Towler, M., & Streek, J.V.D. (2006). Mercury: visualization and analysis of crystal structures. *Journal of Applied Crystallography*, 39(3), 453-457.
- [7] Institute, C.a.L.S., *Methods for dilution antimicrobial susceptibility tests for bacteria that grow aerobically; approved standard*. 2006: Wayne, PA: CLSI.
- [8] Institute, C.a.L.S., *Reference method for broth dilution antifungal susceptibility testing of yeasts; approved standard*. 2002: Wayne, PA: CLSI.
- [9] Frisch, M., Trucks, G., Schlegel, H.B., Scuseria, G., Robb, M., Cheeseman, J., Scalmani, G., Barone, V., Mennucci, B., & Petersson, G. (2009). Gaussian 09, revision a. 02, gaussian. Inc., Wallingford, CT, 200.
- [10] Polishchuk, A.V., Karaseva, E.T., Emelina, T.B., Cramariuc, O., & Karasev, V.E. (2011). Polymorphism and intramolecular proton transfer in fluoroquinolone compounds. *Journal of Fluorescence*, 21(6), 2117-22.
- [11] Krygowski, T.M. (1993). Crystallographic studies of inter- and intramolecular interactions reflected in aromatic character of π -electron systems. *Journal of Chemical Information and Computer Sciences*, 33(1), 70-78.
- [12] Gece, G. (2008). The use of quantum chemical methods in corrosion inhibitor studies. *Corrosion Science*, 50(11), 2981-2992.
- [13] Sahoo, S., Chakraborti, C.K., & Behera, P.K. (2012). Spectroscopic investigations of a ciprofloxacin/hpvc mucoadhesive suspension. *International Journal of Applied Pharmaceutics*, 4(3), 1-8.
- [14] Sadeek, S.A. (2005). Synthesis, thermogravimetric analysis, infrared, electronic and mass spectra of Mn (II), Co (II) and Fe (III) norfloxacin complexes. *Journal of Molecular Structure*, 753(1-3), 1-12.
- [15] Sadeek, S.A., Refat, M.S., & Hashem, H.A. (2006). Complexation and thermogravimetric investigation on tin (II) and tin (IV) with norfloxacin as antibacterial agent. *Journal of Coordination Chemistry*, 59(7), 759-775.
- [16] Zordok, W.A. (2014). Interaction of vanadium (IV) solvates (L) with second-generation fluoroquinolone antibacterial drug ciprofloxacin: Spectroscopic, structure, thermal analyses, kinetics and biological evaluation (L= An, DMF, Py and Et3N). *Spectrochimica Acta Part A: Molecular and Biomolecular Spectroscopy*, 129, 519-536.
- [17] Acar, B., Yilmaz, I., Çalışkan, N., & Cukurovali, A. (2017). Experimental and theoretical studies of the molecular structure of 7-Methyl-3-[(3-methyl-3-mesityl-cyclobutyl)-5-phenyl-5H-thiazolo[3,2- α]pyrimidine-6-carboxylic acid ethyl ester. *Journal of Molecular Structure*, 1139, 130-136.
- [18] O'Boyle, N.M., Tenderholt, A.L., & Langner, K.M. (2008). cclib: a library for package-independent computational chemistry algorithms. *Journal of Computational Chemistry*, 29(5), 839-45.
- [19] Neugebauer, U., Szeghalmi, A., Schmitt, M., Kiefer, W., Popp, J., & Holzgrabe, U. (2005). Vibrational spectroscopic characterization of fluoroquinolones. *Spectrochimica Acta Part A: Molecular and Biomolecular Spectroscopy*, 61(7), 1505-17.
- [20] Lambert, P. (2002). Mechanisms of antibiotic resistance in *Pseudomonas aeruginosa*. *Journal of the royal society of medicine*, 95(Suppl 41), 22.
- [21] Rapa, R.A., Islam, A., Monahan, L.G., Mutreja, A., Thomson, N., Charles, I.G., Stokes, H.W., & Labbate, M. (2015). A genomic island integrated into recA of *Vibrio cholerae* contains a divergent recA and provides multi-pathway protection from DNA damage. *Environmental microbiology*, 17(4), 1090-1102.
- [22] Tan, Z., Tan, F., Zhao, L., & Li, J. (2012). The synthesis, characterization and application of ciprofloxacin complexes and its coordination with copper, manganese and zirconium ions. *Journal of Crystallization Process and Technology*, 2(02), 55.